

An experimental study of cellular detonations in gaseous dodecane/air mixtures

L. Vilasi^a, B. Le Naour^b, P. Vidal^a and V. Rodriguez^a

^aInstitut Pprime, UPR 3346 CNRS, 86961 Futuroscope-Chasseneuil, France

^bMBDA, Route d'Issoudun, 18020 Bourges, France

1 Introduction

Achieving detonation in mixtures of long-chain hydrocarbon fuels with air or oxygen is of practical interest for advanced propulsion systems designed to use pressure gain for more efficient combustion, such as rotating detonation engines. Several fundamental experimental studies of such fuels in vapor or droplet form are available. For example, Tieszen and Stamps [1] report on the detonability and cell widths of several long-chain hydrocarbons vaporized in air. They suggest a relationship between molecular structure and cell size, i.e. the greater the number of cycles, double bonds, or nitrogen atoms in the molecule, the smaller the cell width. However, high densities appear to be detrimental. The detonation of JP-10 in air has been the subject of several studies, including data on cell width by Austin and Shepherd [2], Sorin et al. [3], and Ciccarelli and Card [4], velocity by Schauer et al. [5], and critical ignition energy by Yao et al. [6].

Dodecane is a convenient kerosene surrogate for laboratory studies. For dodecane in air, Veysiere et al. [7] report on detonations in non-preheated sprays of dodecane, up to the droplet diameter of 8 μm . Cammarota et al. [8] report on the effect of the vapor temperature on the detonation properties in vaporized dodecane up to the pyrolysis temperature of 433K.

This work is an experimental analysis of the initiation and the cellular structure of detonations in mixtures of gaseous dodecane and air at several initial temperatures and pressures, based on high-speed shadowgraphs, dynamic pressure measurements, and soot-foil recordings.

2 Experimental methodology and setup

The detonation channel consists of two main elements, namely the driver section and the test section, separated by a Mylar foil (Fig.1). The method involves initiating a detonation in the driver gas using a spark plug and a 700 mm long Shchelkin spiral to accelerate the transition to a steady detonation. When the impact occurs, the Mylar foil acts as a piston, and its sudden movement generates a shock that may or may not trigger detonation in the test gas, depending on its initial properties, namely the equivalence ratio, pressure, and temperature. The interest of the shock-to-detonation process is that it ensures detonation initiation over shorter distances compared to the deflagration-to-detonation transition enhanced by a Shchelkin spiral.

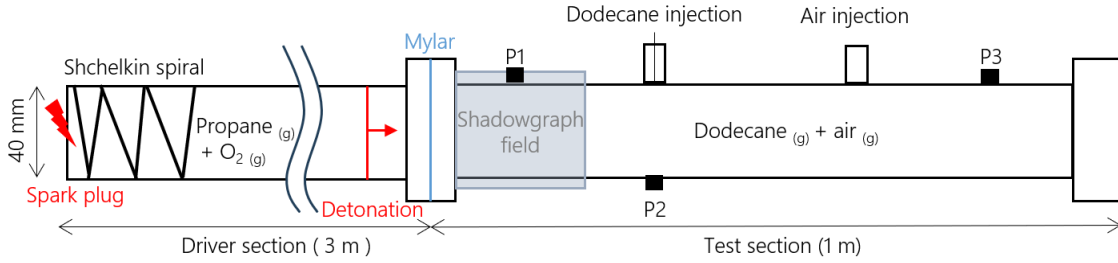


Figure 1: Scheme of the experimental setup

The driver and test sections were 3 and 1 m long, respectively, with the same 40×40 mm² square cross-section. The driver gas was the stoichiometric propane/oxygen mixture $C_3H_8+5 O_2$ at ambient temperature ~ 293 K and at initial pressure p_{driver} 60 kPa or 80 kPa, depending on the conditions in the driver section. The Mylar foil was 18 μ m thick. The mixture in the test section was gaseous dodecane and air at different equivalence ratios ER, initial pressure p_0 and temperature T_0 . Specifically, the fuel studied is a mixture of dodecane isomers, containing in particular 2,2,4,6,6-pentamethylheptane, also known as iso-dodecane, and n-dodecane.

The liquid dodecane was injected into the test section using a microliter syringe to ensure precise volume control. The entire surface of the test section was covered with a silicon blanket embedding heating resistors capable of raising initial temperatures up to 473 K. Heating was regulated using a proportional integral derivative controller (PID). Temperature was measured at the walls, using PT100 sensors (RTD) positioned at the external wall, and inside the chamber, using a 0.5 mm thermocouple (type K, RS Pro), to ensure that the initial temperature T_0 in the test section was homogeneous.

The detonation velocities and pressures in the test section were obtained using three 603B Kistler pressure transducers (Fig.1, P1, P2, P3, 1- μ s response time, 300-kHz natural frequency), each coupled to a Kistler 5018 A electrostatic charge amplifier (200 kHz band width). The distance between P1 and P2 was 25 cm, and 50 cm between P2 and P3. The cellular structure of the detonation was recorded on soot-foils positioned on the bottom wall of the test section. The foils covered the entire length of the wall to provide an additional criterion of detonation steadiness based on constant average cell properties. The detonation initiation and propagation were visualized using high-speed shadowgraphy implemented with a HPVX-2 high-speed camera (acquisition frequency 2 MHz, exposure time 200 ns).

Because of the evaporation process, ER, T_0 and p_0 are not independent. In our experiments, we have fixed T_0 and p_0 and determined the maximum value of $ER(T_0, p_0)$ imposed by the condition of complete evaporation of dodecane. We measured the saturated vapor pressure of dodecane for the 4 values of T_0 323, 333, 343, and 353 K. The saturated vapor pressure is related to the mole fraction of dodecane in the mixture x_{dod} , and thus to ER. The test section is a closed volume, so the maximum fraction of fuel evaporated in the medium of total pressure p_{tot} is

$$x_{dod} = \frac{p_{dod}}{p_{tot}} = \frac{p_{sat,dod}(T_0)}{p_{tot}}, \quad (1)$$

and, therefore, the maximum value ER_{max} of ER that can be obtained by evaporation is

$$ER_{max} = \left. \frac{n_{air}}{n_{dod}} \right|_{st} \frac{x_{dod}}{1 - x_{dod}} = \left. \frac{n_{air}}{n_{dod}} \right|_{st} \frac{\frac{p_{sat,dod}(T_0)}{p_{tot}}}{1 - \frac{p_{sat,dod}(T_0)}{p_{tot}}}. \quad (2)$$

Figure 2 shows the curves of $ER_{\max}(T_0, p_0)$ as a function of p_0 depending on T_0 . For example, the value $ER=1$ can be obtained only for values of p_0 lower than 50 kPa. In our experiments, we varied p_0 from 30 to 100 kPa, and T_0 from 313 to 353 K.

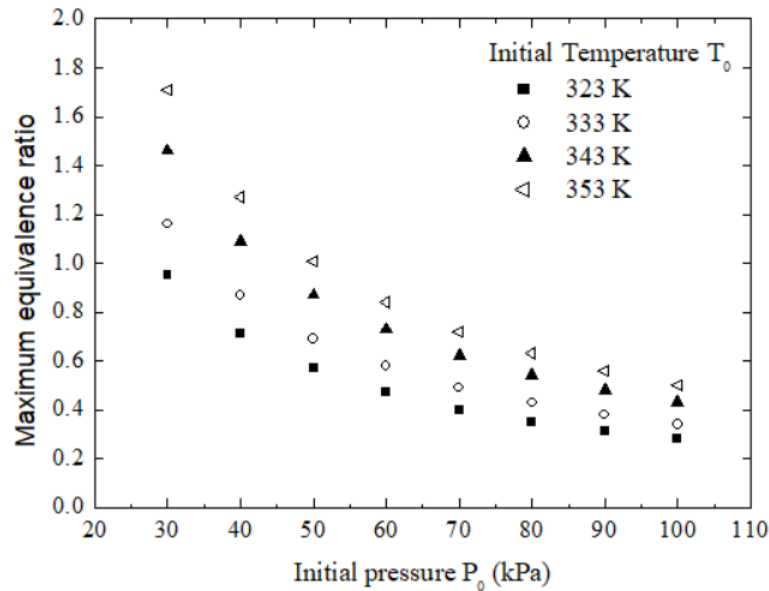


Figure 2: Maximum values $ER_{\max}(T_0, p_0)$ of ER for dodecane/air mixture obtained by evaporation, for different p_0 and T_0

3 Results and analysis

Figure 3 shows shadowgraph images of shock initiations in the dodecane/air mixture at $ER = 1$, $p_0 = 40$ kPa, $T_0 = 353$ K for the two driver initial pressures p_{driver} 60 kPa (left) and 80 kPa (right), with time increasing from top to bottom. The top images show the local explosion that indicates the beginning of initiation. Figure 3a (left) corresponds to the lower initial pressure of 60 kPa in the driver section and shows a delayed detonation initiation, originating from the top wall. Figure 3b (right) corresponds to the higher initial pressure of 80 kPa in the driver section and shows quasi-immediate detonation initiation, at the center of the test cross-section. The closest pressure transducer (P1) is located slightly behind the explosion locus and indicates a pressure of 2.2 MPa. The soot recording on the bottom wall of the test section shows cells with essentially constant properties from a few centimeters after the position of transducer P2. Because the distance of 50 cm between transducers P2 and P3 is much greater, we considered the detonation was steady between P2 and P3, with average velocity of 1950 ± 10 m/s.

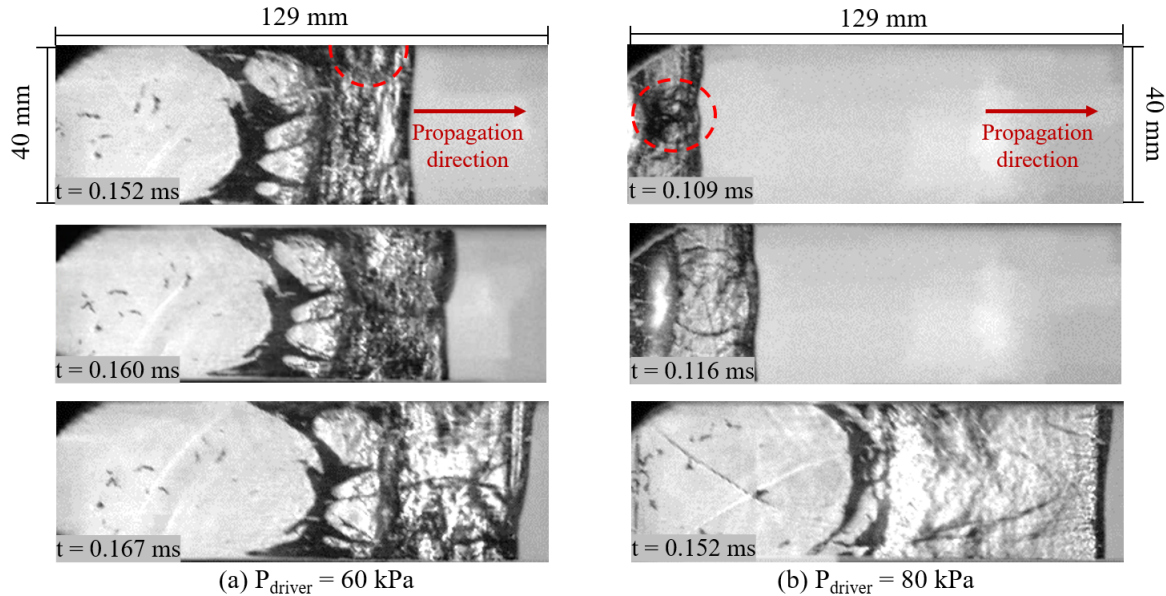


Figure 3: Shadowgraphy of detonations in the stoichiometric dodecane/air mixture ($ER = 1$). $p_0 = 40$ kPa, $T_0 = 353$ K

Figure 5 shows a longitudinal recording of the cell structure of a dodecane/air detonation for $p_0 = 30$ kPa, $T_0 = 333$ K, $ER = 1$. The two plates are from the same experiment, time increasing from top to bottom, the left side of the bottom plate continuing the right side of the top plate. The recording shows that the detonation is initiated ~ 4 cm after the beginning of the first plate, slightly before the position of transducer P1. The cells immediately after initiation are very small and relax to a larger size of approximately 8.6 ± 1.2 mm. The histogram in Figure 4 shows that these relaxed cells can be considered as regular [9–11]. For the conditions considered, we calculated the Chapman-Jouguet velocity D_{CJ} and pressure p_{CJ} using the same ZND computer program as in [12] and the MURI 2 chemical kinetic mechanism [13], and found the values $D_{CJ} = 1777$ m/s and $p_{CJ} = 0.4$ MPa. Between sensors P1 and P2, the detonation appears to be overdriven, with the measured value of velocity $D = 2212 \pm 10$ m/s $> D_{CJ}$ (Fig. 6). Between P2 and P3, the measured velocity of $D = 2036 \pm 10$ m/s is 15% higher than D_{CJ} . The fact is that the detonation is still overdriven at the P2 position, as the cell widths there are smaller than at the P3 position, so that the mean velocity between P2 and P3 is necessarily higher than D_{CJ} . The soot recording in Figure 5 shows a number of cells in the transverse dimension of about 5. This is too small to assume that the cells are independent of this dimension, so we have not attempted to use our model for predicting intrinsic and significant mean cell widths [12] for these conditions. Finally, we indicate that for the same p_0 and ER , the higher T_0 , the earlier the detonation initiation.

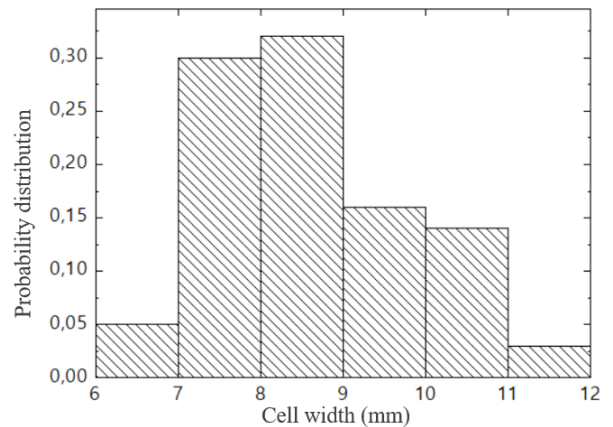


Figure 4: Cell width distribution for the detonation in the stoichiometric dodecane/air mixture ($ER = 1$). $p_0 = 30$ kPa, $T_0 = 333$ K

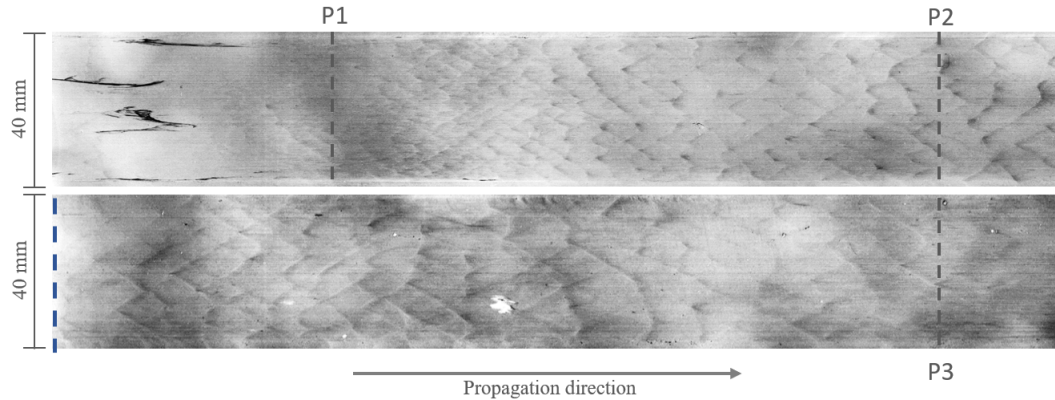


Figure 5: Cellular structure in dodecane/air mixture ($ER = 1$). $p_0 = 30$ kPa, $T_0 = 333$ K

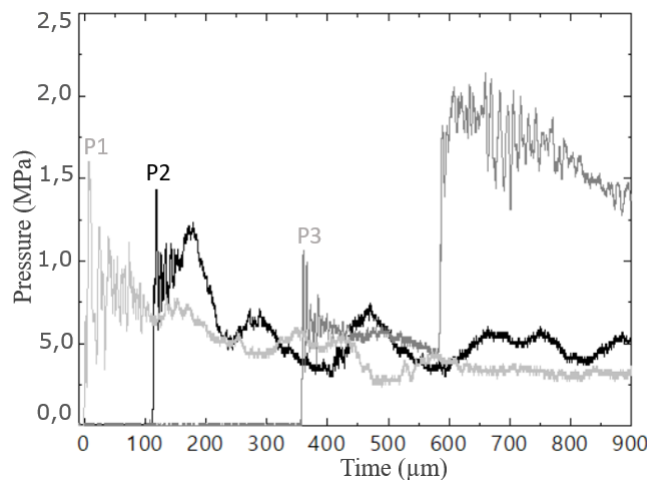


Figure 6: Pressure signals in the stoichiometric dodecane/air mixture ($ER = 1$). $p_0 = 30$ kPa, $T_0 = 333$ K

4 Discussion and conclusion

This work presents results on the initiation, the propagation and the cellular structure of detonation in a gaseous dodecane/air mixture at several initial equivalence ratios, temperatures and pressures. Steady propagation was obtained for initial pressures ranging from 30 to 100 kPa, with ER greater than 0.6.

Detonation velocity, pressure, cell width and ignition positions were measured for several initial conditions. The cell structure appears to be regular on the sidewall recordings. However, the number of cells in the transverse dimension of the channel is too small to consider the geometric properties of these cells as independent of this dimension. An increase in initial pressure, or a wider channel for the same initial pressures as in this work, would be required to overcome the influence of confinement on the cell structure.

Detonation properties with equivalence ratios $ER=1$ for pressures above 50 kPa remain to be investigated, requiring higher initial temperatures than at the time of this writing. To this end, ongoing work focuses on suppressing the temperature difference between the ends and the center of the test section by using a longer silicon blanket. The results will be presented in the oral session and will include the dependence of cell width on temperature and equivalence ratio.

Acknowledgements

This work was financially supported by the Agence de l’Innovation de Défense and MBDA France.

References

- [1] S. Tieszen and D. Stamps (1991). Gaseous hydrocarbon-air detonation. *Combustion and Flame*. 84: 376-390.
- [2] J.M. Austin and J.E. Shepherd (2003). Detonations in hydrocarbon fuel blends. *Combustion and Flame*. 132: 73-90.
- [3] R. Sorin, P. Bauer, D. Desbordes (2008). Detonability of THDCPD-exo-air mixtures. *Shock Waves*. 17: 363-369.
- [4] G. Ciccarelli and J. Card (2006). Detonation in Mixtures of JP-10 Vapor and Air. *AIAA Journal*. 44: 362.
- [5] F. Schauer, C. Miser, C. Tucker, R. Bradley and J.Hoke (2012). Detonation Initiation of Hydrocarbon-Air Mixtures in a Pulsed Detonation Engine. *AIAA Journal*.
- [6] G.Yao, B. Zhang, G. Xiu, C. Bai and P. Liu (2013). The critical energy of direct initiation and detonation cell size in liquid hydrocarbon fuel/air mixtures. *Fuel*. 113: 331-339.
- [7] B. Veyssiere, B.A. Khasainov, M. Mar and M.A. Benmahammed (2013). Investigation of Detonation Propagation Regimes in Liquid Sprays. 24thICDERS, Taiwan.
- [8] F. Cammarota, A. Di Benedetto, V. Di Sarli, E. Salzano (2019). Influence of initial temperature and pressure on the explosion behavior of n-dodecane/air mixtures. *Journal of Loss Prevention in the Process Industries*. 62.
- [9] R. A. Strehlow (1964). Reactive Gas Mach Stems. *Physics of Fluids*. 7: 908-910.
- [10] V. I. Manzhalei, V. V. Mitrofanov and V. A. Subbotin (1974). Measurement of inhomogeneities of a detonation front in gas mixtures at elevated pressures. *Combustion, Explosion and Shock Waves*. 10: 89-95.
- [11] M. Short and G. J. Sharpe (2003). Pulsating instability of detonations with a two-step chain-branching reaction model : theory and numerics. *Combustion Theory and Modelling*. 7: 401-416.
- [12] V. Monnier, P. Vidal, V. Rodriguez and R. Zitoun (2023). From graph theory and geometric probabilities to a representative width for three-dimensional detonation cells. *Combustion and Flame*. 256, 112996.
- [13] T. Malewicki, S. Gudiyella and K. Brezinsky (2013). Experimental and modeling study on the oxidation of Jet A and the n-dodecane/iso-octane/n-propylbenzene/1,3,5-trimethylbenzene surrogate fuel. *Combustion and Flame*. 160: 17-30.